ELSEVIER

Flow Measurement and Instrumentation 13 (2002) 237–245

Flow Measurement and Instrumentation

www.elsevier.com/locate/flowmeasinst

Large scale PIV-measurements at the surface of shallow water flows

V. Weitbrecht *, G. Kühn, G.H. Jirka

Institute for Hydromechanics, University of Karlsruhe, 76128 Karlsruhe, Germany

Abstract

To measure the flow dynamics at the surface of shallow water flows over a large measuring field, a simple and reliable method has been developed using the advantages of Particle Image Velocimetry (PIV). Besides the determination of mean flow conditions and turbulent flow characteristics, this method makes it possible to track two-dimensional large coherent structures, which are the dominating flow phenomena in many shallow flow applications. As basic equipment, a commercial PIV software system has been used. The measurements are carried out at the water surface, which means that no laser light sheet is needed. Depending on the time scales of the flow and camera characteristics, it is even possible to work with a constant light source. A particle dispenser to provide a homogeneous distribution of particles on the water surface is also presented. Because floating particles have a strong tendency of sticking together, different types of particles and special coatings have been tested to reduce this problem. A laboratory application of this method is presented to analyze the effects of shallow dead-water zones on exchange processes in rivers where large coherent two-dimensional flow structures in the mixing layer dominate the flow characteristics.

Keywords: Large scale PIV; Shallow flows; Grain fields; Particle dispenser

1. Introduction

In shallow flow problems velocity information with high spatial and temporal resolution is needed to understand the dynamics of the flow and the related mixing processes. Shallow flow phenomena can be found in rivers, coastal zones or the atmosphere, where the dominating processes are two-dimensional [1]. Large coherent motions, that are inititated, for instance, in shallow wake flows behind obstacles [2] or in shallow mixing layers [3–5] strongly influence the dynamics of such a system and are, therefore, a determining factor for the mixing and transport processes. Measurement of the velocity field describing the generation and the evolution of these coherent motions is the major aim of this investigation.

To simulate shallow flows under laboratory conditions, scaling effects limit the minimum dimensions and velocities such a model may have. For example, it it necessary that viscous forces do not influence the flow much more than in the natural flow. This restriction leads to scale models where the measurement area is on the order of meters.

The fundamental properties of shallow flows can be obtained by measuring surface velocities because of the two-dimensional behaviour of these flows. Moreover, the horizontal length scales of the coherent structures in these flows are much larger then the vertical extent of the flow, which means that the dominating processes are in the horizontal plane. The flow structure in vertical direction of shallow flows can be determined using the measured surface velocities and adapting known vertical velocity profiles, such as those determined by Blasius for open channel flow [6], or for turbulent jets in shallow water [7].

In the present study PIV has been used to measure velocity fields at the water surface. PIV constitutes a powerful technique to perform two-dimensional quantitative measurements for a large variety of flows [8,9]. Many investigations have been made to improve the performance of PIV in the past by developing new correlation methods [10] or improving the image processing [11]. These efforts have lead to “off the shelf” PIV-packages that are easy to adapt for different application.

* Corresponding author. Tel.: +49(0)721/6087682; fax: +49(0)721/661686.

E-mail address: weitbrecht@ifh.uka.de (V. Weitbrecht).

0955-5986/02/$ - see front matter
PII: S0955-5986(02)00059-6

Compared to standard PIV applications where measurements are carried out within the water body using a laser light sheet to illuminate the measuring plane [12–14], surface PIV measurements are relatively straightforward because no laser is needed. In this case the measuring plane is given by the water surface which means that for illumination, standard flood lights can be used, provided that the water surface is not strongly disturbed by wave motions. To keep the developed system flexible, a commercial PIV package including camera, frame grabber, and controlling and evaluation software has been used, with special adaptation to the large scale laboratory problem. PIV measurements in large measuring areas have been performed in former investigations by Linden et al. [15] and Tarbouriech et al. [16] in rotating tanks with stratified flow conditions. In both cases the measurements have been performed using a light sheet to illuminate the measuring plane. Uijttewaal [17] presented particle tracking measurements at the water surface where the particles were distributed manually on the water surface. In Uijttewaal et al. [18], measurements can be found using the presented method, where the influence of grid turbulence on shallow flows were determined. Von Carmer et al. [19] were using the presented technique to analyze shallow wake flows.

Measurements of velocity fields in large areas with high spatial and temporal resolution are difficult because of the problem of homogeneous particle seeding on the water surface. To solve this problem a particle dispenser (see Section 2) has been developed which can be mounted a short distance upstream of the measurement area over the water surface. A second major problem relates to the tendency of most floating particles to agglomerate. This phenomena leads to a distorted particle distribution which means that in some regions no particles are found while in other regions large particle aggregations are floating on the water surface. A study of different particle materials and special coatings to reduce agglomeration is presented in Section 2. In Section 3 the results are given of different tests that evaluate the accuracy of the presented method.

In Section 4 measurements are presented where the system has been applied to a laboratory problem. In these experiments exchange processes between dead-water zones and the main stream of a river have been investigated to determine the influence of these zones on the transport characteristics of the river. First, the mean flow conditions are presented to visualize the recirculating water body. Second, the turbulent motion representing the fluctuating part of the water motion are presented in order to characterize the mixing layer between the dead-water zone and the main stream. Finally, vorticity fields to analyze the coherent motion of the flow in the mixing layer are determined.

2. Elements of the measuring system

In the following section the different parts of the measuring system, PIV-package, camera, particles, particle dispenser, and illumination, are described.

The acquisition and analyzing system represents a standard PIV-package from La Vision® including PC, PIV and control software, PIV-camera, frame-grabber and programmable-timing-unit (PTU) (Fig. 1). The PTU is a PC integrated timing board that allows a precise time management for the trigger pulses needed to control camera and illuminations, like a laser or strobe light. The PC is equipped with 1 GB RAM that is used to store the images before shifting them to the hard disk. Therefore, the RAM is the limiting factor for the length of a time series. To control the capturing process and the analysis of the images the software package DaVis provided by LaVision was used. DaVis includes algorithms for PIV and PTV evaluation. While the PTV-algorithm attempts to track every particle from one image to the next, the PIV-algorithm is based on a standard cross-correlation via Fast Fourier Transformation [8] between two images. For the cross-correlation the image is divided into small interrogation areas resulting in one displacement vector for each area. Detailed information can be found in Raffel et al. [9]. Because the dynamic range of the velocities in open-channel flows can be very high, a simple PIV-algorithm would fail. In this case an adaptive multipass processing tool is available, where the PIV-algorithm starts with a large interrogation area and uses the obtained velocity as reference velocity for the next smaller interrogation areas [11]. Algorithms to invert the images before pre-processing were added to the standard DaVis suite. One limitation of the PTV package is that only 16 000 particles are supported per image.

The Imager 3 camera, Sensicam, with a 1/2inch-CCD-sensor, has a resolution of 1280×1024 pixels with a gray scale resolution of 12 bits. With a pixel clock of 12.5 MHz, frame-rates up to 8 Hz are possible. The cam-

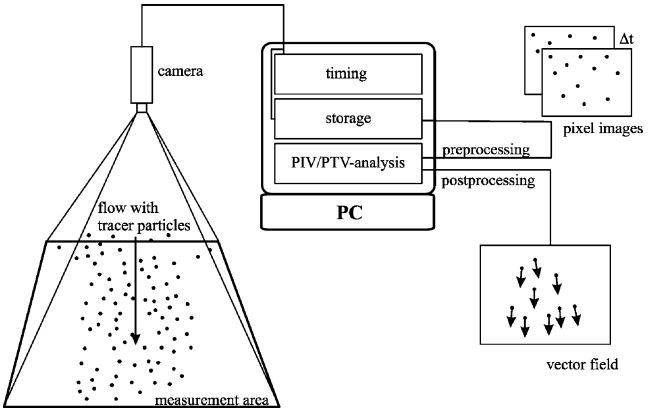

Fig. 1. Schematic sketch of a PIV-system.

era can be operated in two different modes. The first mode is a single frame-mode. In this mode every image is read out after it is captured, so that the time distance between every image is the same. If the flow field is slow enough this mode can be used, and 7 velocity fields per second can be obtained. For flows with higher velocities the double frame mode has to be used. In this mode two images are captured within a very short time. The first image is not read out but shifted to the storage position on the chip and then the second frame is captured. The shortest time allowed between the two frames is 400 ns. During the transfer of these two frames to RAM a read out-time of 125 ms is necessary. A measurement series of 4 double frames per s, therefore, leads to 4 velocity fields per s. For the chosen camera (Imager 3), a specialized, camera-specific framegrabber is used. Camera and frame-grabber are connected with a fiber-optic so that distances between both elements of more than 10 m can be realized.

To capture large measurement planes while the space above the experiment is limited to a maximum of 3 m, an f-mount, 15 mm wide angle lens (NIKON) with very small distortion errors was used. This lens provides a very good resolution combined with high luminosity.

A difficult part of the experimental setup is the choice of proper tracer particles. The particles have to fit different requirements to be applicable. In our case of surface velocity measurements the tracer particles have to swim at the water surface so that the material has to be somewhat lighter than water. Particles which are too light can be affected by air flow above the water surface.

In Table 1 the properties of the tested tracers are listed. All of these tracers float on the water surface. Polystyrene was too light; the airflow above the surface had too big an influence on the floating particles. Polyethylene (PE) and Polypropylene (PP) have a density of 0.9 g/cm^3, which worked very well.

Another important point is the size of the particles. Particles which are too small cannot be seen by the camera or will evoke peak-locking effects (see Section 3). To avoid this Raffel et al. [9] suggest using particles with a diameter bigger than 1.5 pixels. Particles which are too big can have the problem of not following the flow structures because of inertial forces. A compromise is given by particle dimensions between 2 to 5 pixels. In the present application the particle diameter was about 2 mm.

Many particle materials have the tendency to form conglomerates on the water surface due to surface tension effects. All of the tested materials show this tendency. However, PE or PP that has been coated with laquer exhibits minmimal agglomeration effects and have been adopted in the presented applications. Also the material color has to have sufficient contrast to the background. Due to a white flume bottom, black particles were needed. Experiments attempted with fluorescent material showed much less contrast.

Summarizing the properties of the different particles, Polypropylene with additional matt black lacquer finish gives the best results. These particles can be purchased by Feddersen & Co., Hamburg, Germany, under the name “Hostacom PPR 1042 12”. A blender was used to add the lacquer finish on the particles so that the particles do not stick together during the drying process.

A homogeneous distribution of particles within the measuring field is important for good results in terms of a closed velocity vector field. A particle dispenser which is able to seed the water surface homogeneously with particles, at a rate that depends on the ambient flow velocity was developed (Fig. 2). The essential part of the dispenser is a roller brush, which is driven by an AC gear motor. The velocity of the brush can be continuously varied between 0 and 5 rpm to control the particle release rate. The brush ensures an equal particle distribution over the whole width. The tracer particles are stored in a container behind the brush. A pneumatic vibrator is installed on the container to ensure a constant particle supply. The pneumatic vibrator shakes the metal wall of the storage container with about 6000 oscillations per minute and a centrifugal force of 50 N. The force and number of oscillation can be adapted to the material and its humidity.

Table 1
Properties of different tracer materials

	(1)	(2)	(3)	(4)	(5)	(6)
material	Polystyrene	coal	wood	expanded clay	PE	PP
form	sphere	die	sphere	sphere	cylinder	cylinder
diameter [mm]	2	1–5	4	1–2	2–3	2–3
density [g/cm^3]	0.04	0.50	0.50	0.73	0.90	0.90
resistance to air flow	−	+	+	+	+	+
avoidance of aglomeration	−	−	o	−	−	o
low cost	o	+	−	+	+	+
durability	+	o	−	+	+	+

− poor, o acceptable, + good.

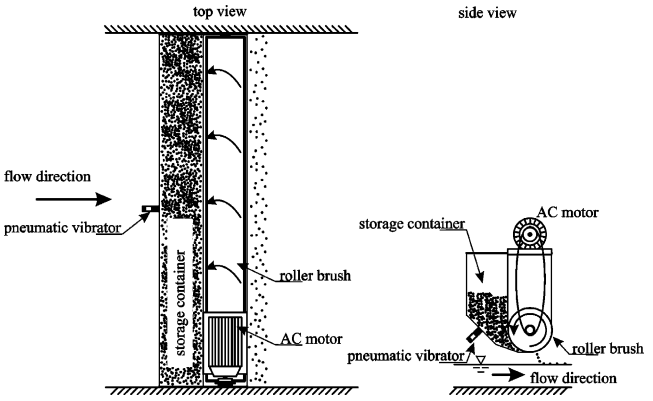

Fig. 2. Schematic sketch of particle dispenser.

The dispenser is located only a few centimeters over the water surface in order to avoid surface waves from falling particles. It is also advisable to place the dispenser close to the measurement plane to minimize the number of conglomerates. The particles are recollected at the end of the flow section and reused, as the number of particles which is needed for such an experiment is quite high.

In the single frame mode (slow flow conditions) the measurement plane is illuminated with constant halogen floodlights. Four 1 KW floodlights were used indirectly, in order to reduce the disturbing effects of shadows and to reach nearly homogeneous light conditions. This means that the floodlights are turned to the ceiling, which is equipped with matt reflection screens. In the double frame mode (fast flow conditions) the shutter is not closed after taking the second image until the frames are read out. In this case a strong stroboscope is used as the light source which can be triggered by the PTU. An external optical sensor is necessary to measure delay times and jitter, in order to adjust the trigger scheme.

3. Accuracy of the measuring system

A common technique to test the accuracy of PIV systems is given by Westerweel [20], where artificial particle clouds are generated with random spatial distribution to simulate a reproducable particle movement under well determined boundary conditions. In the present case the particle clouds were plotted on white paper and mounted on a 3-D positioning system below the CCD camera. This positioning system is able to do stepwise movements with an accuracy of 0.0125 mm. With the aid of this setup the measurement accuracy of the complete system including the camera was determined dependent on particle size and density. Furthermore the influence of the displacement between two images and finally the influence of a tilted camera were tested.

Tests using particles of different size showed, that the minimal value of the particle diameter had to be at least 1.5 pixels in order to avoid peak-locking effects. Smaller particles lead to particle displacement distributions in a vector field that contains strong peaks at the position of integer pixel displacement (Fig. 3) [9,21].

Raffel et al. [9] showed that particle concentration influences the probability of detecting the valid displacement as well as the measurement uncertainty. Tests with changing particle concentration showed that the number of particles in each interrogation area should be higher than 5. The dispenser operation satisfies this criterion.

Tests to determine the influence of the particle displacement showed, that the maximum particle displacement between two frames should be less then 50% of the interrogation area. For higher flow velocities the camera frame rate has to be increased. In the cases of very high velocities the camera has to be used in the double shutter mode using stroboscopic illumination. If the dynamic range of the flow is too high, additional tools like the adaptive multipass function have to be used.

Every image contains a certain distortion which is caused by the camera lens. By tilting the camera towards the vertical, an additional error due to distortion effects has to be eliminated. These effects are minimized using a polynomial calibration of third degree in the x and y directions. It should be noted that this procedure increases the noise, which has a certain influence on the turbulent flow characteristics. Stronger tilting angles can only be handled by using additional optical components, like a Scheinpflug optic.

Turbulent flows are characterized by random motions of different length and time scales. If a particle ensemble is transported within such a flow it will get distorted due to shear. If the distortion in an interrogation area evoked by the velocity shear is too high the cross correlation of the PIV evaluation can fail. Tests have been made where every interrogation area of the second frame is rotated by a certain angle (Fig. 4) in order to determine the

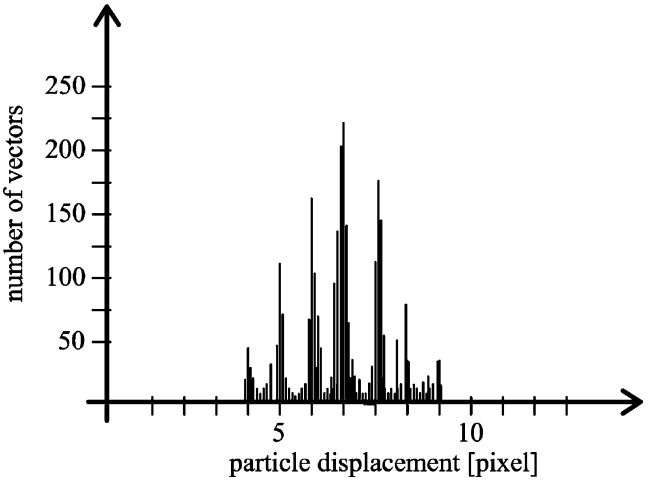

Fig. 3. Illustration of peak locking effect associated with insufficient particle image size, by showing a histogram of PIV displacements.

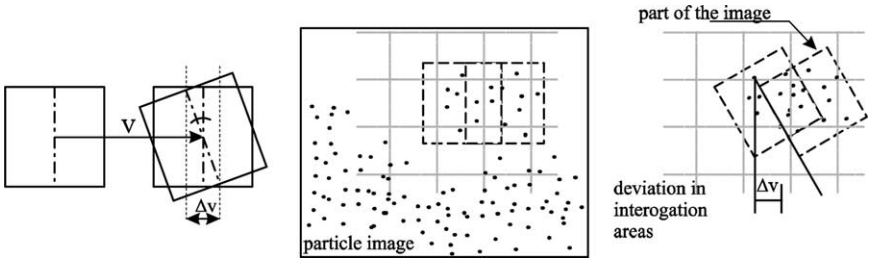

Fig. 4. Rotation of interrogation areas.

influence of velocity shear. Fig. 5 shows that there is a dependency of the mean flow velocity to the rotation angle.

The evaluation of the spatial standard deviation shows that additional noise generates these motions due to the rotation of the interrogation area. Grant [22] proposed as a quality criterion

$$\frac{\Delta u}{U} = \frac{\Delta v}{V} < 0.2 \tag{1}$$

with Δu and Δv as the velocity gradient in x- and y-direction and U and V the mean velocity in x- and y-direction, which was verified in the present study.

Another test was performed where the particle plots were mounted on a rotating disc with a constant angular velocity, in order to control the measured mean velocities. In Fig. 6a it can be seen that that the measured values fit very well to the theoretical value. The strong deviations on the left hand side arise because the measurement plane was not exactly centered to the camera, so that on this side areas without particles are traveling through the measurement plane. Neglecting the left border, the deviation of the displacement from its theoretical value is less then 0.5 pixels as shown in Fig. 6b.

Image-preprocessing can also effect the accuracy. In the present case the pictures are first inverted and then filtered using a high-pass filter, which eliminates the background structures. Additional noise reduction by subtracting an offset value can make the measurements more accurate. An additional effect of these procedures is that the resulting pictures can be compressed much more efficiently, which saves a lot of storage capacity.

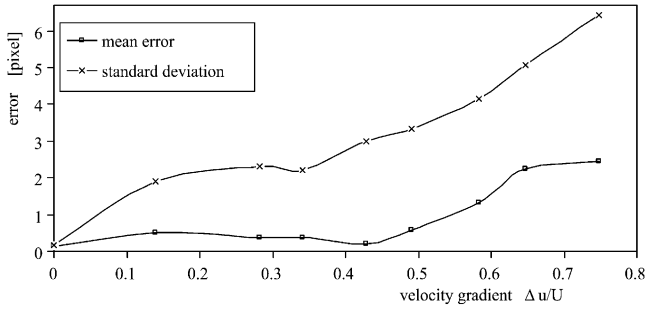

Fig. 5. Accuracy of pixel displacement, related to the velocity gradient in an interrogation area.

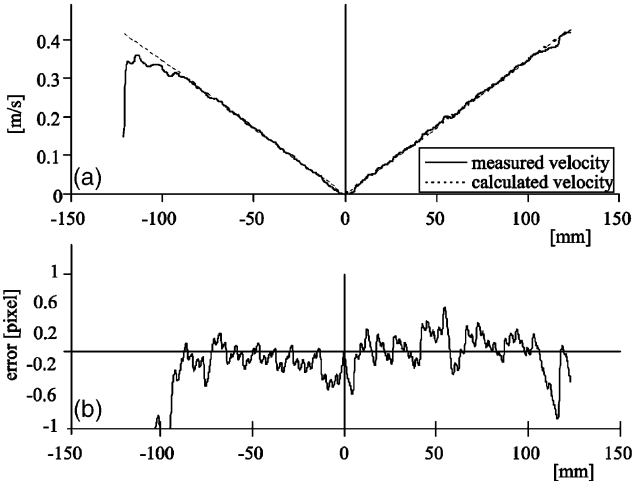

Fig. 6. Rotating disk tests: (a) Measurements of the velocity distribution, (b) deviation from calculated velocity.

In summary, the systematic error of the measurement method is less than 0.5 pixels displacement [23]. The results are very sensitive, however, to different pre- and postprocessing parameters. Results can be obtained from every image pair. For each experimental setup, the parameters have to be adjusted carefully to the existing conditions like flow velocity, size of the measurement plane and illumination.

4. Application

Results are presented here where the developed method has been used to analyze the flow dynamics in a mixing layer between dead-water zones formed by groin fields and the main stream of a river. This is part of a research project dealing with exchange processes and their influence on longitudinal dispersion of dissolved tracer material in rivers [24]. The flow in this application is quasi two-dimensional [25] because of a very high width/depth ratio of the flow, which means that the flow is very shallow. Large coherent structures that emerge at the groin heads dominate the flow and the associated mixing processes. This fact enables us to use the proposed method to measure only the surface velocities to characterize the flow.

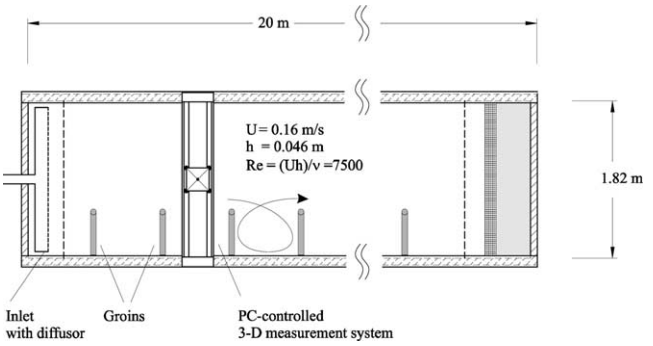

Fig. 7. Schematic sketch of the experimental setup.

The laboratory experiments were conducted in a 20 m long and 1.81 m wide tilting flume, where one side of the flume (Fig. 7) is intended to represent the channel mid section and the other side the river bank including the groin fields. The water depth was $h = 0.046$ m, and the mean flow velocity in the main channel was $U = 0.16$ m/s, which leads to a bulk Reynolds number $(Uh)/\nu$ of about 7500. The groin length is 0.5 m and the distance between two groins is 1.25 m which leads to an aspect ratio of 0.4 which is typical for groin regulated rivers [26].

The flow in the dead-water zone is characterized by slow recirculating motions (Fig. 8) formed by a system of two separate gyres. One large gyre in the center of the dead-water zone dominates the flows, while a small counter-rotating gyre lies in the upstream corner of the dead-water zone. This second gyre is rotating much slower than the first gyre. Between the main stream and dead-water zone a mixing layer develops which is dominated by coherent structures. These structures are generated at the groin head and grow during their travel between two groins, much stronger in the horizontal than in the vertical direction. Because mass exchange processes are dominated by these large coherent motions, they have to be analyzed by a technique that captures the spatial details, such as large scale surface PIV technique.

The camera was mounted 3 m above the water surface which leads to a measurement plane of 1.5 m × 1.2 m. With a camera resolution of 1280 × 1024, one pixel is equal to 1.2 mm in the measurement plane. As the diameter of the floating particles is about 2.5 mm, every particle is represented by at least 4 pixels on the camera chip. To measure the surface velocities a set of 3 runs containing 200 pictures each were captured providing 597 vector fields with a resolution of 60 × 84 vectors (Fig. 8b). The camera frame rate was chosen to be 7 Hz representing a time series of 85 s. The limiting factor of the length of a series is given by the main memory of the PC and the storage capacity of the hard drive.

The raw picture frames were preprocessed by the following procedure to raise the efficiency of the cross-correlation process. First, the pictures were inverted because pictures with a black background can be compressed more efficiently. In a second step, a sliding minimum filter was used to eliminate long wave illumination changes due to the background and to amplify the presence of the particles. As a third step, noise is reduced by subtracting an offset value in the magnitude of 1 per cent of the maximum value. For the PIV evaluation the following settings were made. The adaptive multipass started with an interrogation area of 64 × 64 pixels and ends at 32 × 32 pixels with an overlap of 50 per cent which leads to a final resolution of 16 × 16 pixels of the vector field. Every vector represents the flow velocity of a 3.8 cm × 3.8 cm field on the water surface.

The resulting vector fields still contain errors that require further postprocessing. First, a quality criterion, known as peak ratio factor, Q, is checked. This factor Q is defined as,

$$Q = \frac{P1-\min}{P2-\min} \tag{2}$$

where min is the lowest value of the correlation plane, and $P1$ and $P2$ are the peak heights of the first and second highest correlation peak. Second, a median filter is used where the deviation of a central vector compared to the root mean square value of the surrounding vectors should be of order 1.5. If this criterion is exceeded this vector is rejected and the vector which is associated with the second order correlation peak is checked and normally will be inserted. The resulting vector fields are stored so that all the following analysis is performed using Matlab.

The primary result of these measurements are instan-

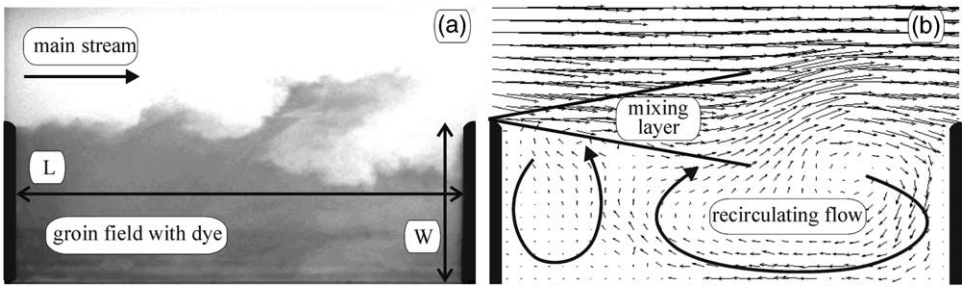

Fig. 8. Flow dynamics in a mixing layer between groin field and main stream, (a) dye experiment, (b) PIV data of an instantaneous velocity field.

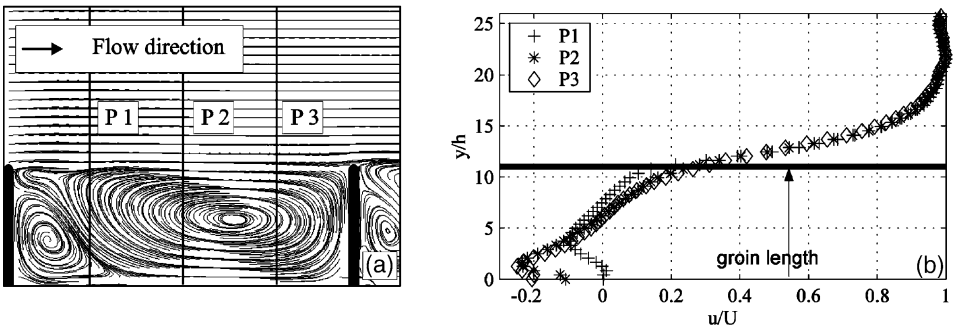

Fig. 9. Mean flow properties, (a) streamlines of flow in the dead-water zone, (b) velocity profiles at 3 different sections of the flow. The velocity profiles are normalized by the water depth h and the main stream velocity *U*.

taneous velocity fields (Fig. 8b) that demonstrate the typical behavior of the flow. The dynamic behavior of the mixing layer can be detected and a first impression of the large coherent structures can be given. In a next step, the mean flow characteristics can be determined by time-averaging over the whole length of the time series. By plotting streamlines for the time-average vector field the two-gyre system can be visualized (Fig. 9a). The mean flow profiles of the *u*-velocity component can be used to characterize the width of the mixing layer and the evolution of the mixing layer between two groins.

Results from former investigations, where velocity profiles over the water depth were investigated, can be used in order to transfer the results obtained at the water surface into flow velocities which are representative for the complete water body. Using the Blasius 1/7-law the mean flow velocity of the depth-integrated velocity profile can be obtained multiplying the surface velocity by a theoretical factor of 0.817. In the presented case the mean flow velocity, calculated by the measured flow rate divided by the main stream area, leads to a factor 0.805. In the region of the mixing layer where the coherent structures are dominant the velocity profiles differ slightly from the Blasius profile. Giger et al. [7] determined a 1/10 law for the vertical velocity profiles in such regions.

The turbulent flow characteristics can be determined in terms of root mean square values to characterize the turbulent characteristics of the flow. In Fig. 10 the rms-values of the transverse component (v') are visualized. The turbulent behavior of the mixing layer is clearly visible. The rms-profiles show that the strongest fluctuations can be found close to the upstream groin in the mixing layer which is related to profile P1.

Laser-Doppler-Verlocimetry (LDA) measurements have been made to compare the measured PIV data. In Fig. 10 the normalized turbulence intensity for profile P2 in the mid section between two groins in comparison to the PIV measurements is plotted. Each point of the P2-LDA profile represents a time series of 2 min with a sampling rate of about 150 Hz. The overall behavior of the rms-profiles shows a good agreement between the PIV and the LDA measurements. Problems occur in the region of low turbulence intensity, where small scale turbulent structures in the main channel dominate. In this region of the flow the maximum turbulent length scales are in the order of the water depth which is 4.6 cm. The resolution of the PIV measurements is in the order of 3.8 cm. To determine the turbulent flow characteristics of the undisturbed channel flow a higher resolution, which means a smaller measurement plane, should be chosen. However, in the present study the main focus was to determine the flow behavior in the mixing layer which is well represented by the PIV measurements.

The PIV measurements have also been used to calculate vorticity fields, which corresponds to the changing orientation in space of a fluid particle [27]. In the present study these quantities are used to visualize and to quan-

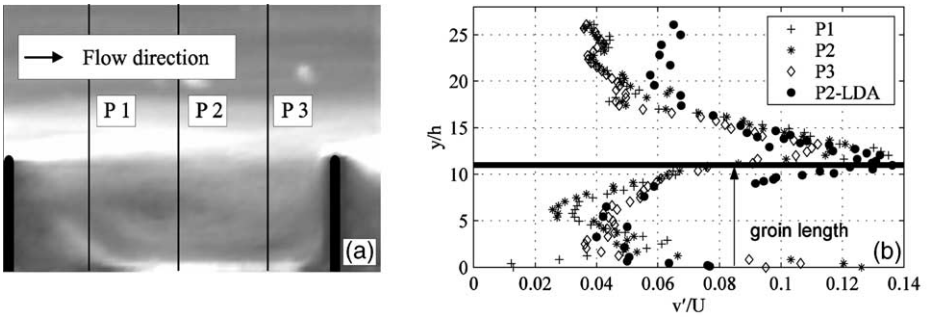

Fig. 10. Turbulent flow characteristics, (a) visualization of the turbulent velocity fluctuations in transverse direction, (b) v' profiles at 3 different sections of the flow field. The values are normalized by the water depth *h* and the main stream velocity *U*.

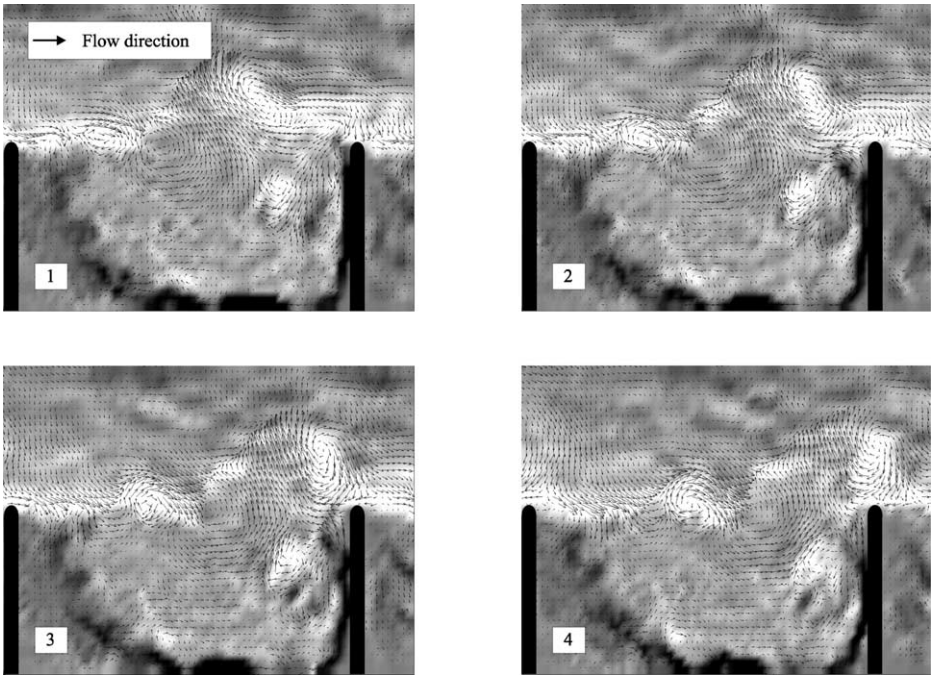

Fig. 11. Series of vorticity fields with time intervals of 1 s. Light color indicates clockwise rotation and dark color anticlockwise rotation.

tify the large coherent motions occurring in the mixing layer between the dead-water zone and main stream. In Fig. 11 the white spots represent motion with clockwise rotation. They are generated at the groin heads and grow because of the strong velocity shear between main stream and dead zone in horizontal direction. Anticlockwise rotation is found in the dead-water zone along the downstream groin and the channel bank as well as in the second mixing layer between the small gyre in the upstream corner of the dead zone and main gyre in the center.

5. Conclusions

Shallow flows are dominated by two-dimensional flow strucutures, which means that the overall behaviour of the flow can be analyzed using surface velocities. To simulate shallow flows under laboratory conditions, facilities have to be used where the horizontal dimensions are in the order of meters. PIV measurements at the water surface, using appropriate techniques to seed the water surface homogeneously with particles of sufficient density, provide a suitable method to analyze the flow dynamics of such flows. Using the water surface as measurement plane, no laser has to be used to provide a light sheet. This makes the presented method considerably less complicated. If particle size and density has been chosen correctly, the accuracy of mean velocities is smaller than 0.5 pixels. In the present study the dynamics of the flow in the case of groin field regulated rivers have been analyzed. It could be shown that the behaviour of the flow is well represented by the surface measurements. Problems arise in regions where the length scales of the turbulent structures are in the order of the PIV resolution. Any other application where the surface velocity represents the behaviour of the overall flow, because the flow is quasi two-dimensional, such as shallow wake flows or confluence problems in rivers, can be analyzed using the presented technique.

Acknowledgements

The authors would like to thank M. Kurzke, K. Schmidhäussler and R. Erler for their help in performing the experiments, as well as M. Ziegler, J. Ulrich and P. Giraud for their technical support. The project was sponsored by the German “Federal Ministry for Education and Research” (bmb+f Grant No. 02 WT 9934/9).

References

[1] D. Chen, G.H. Jirka, Experimental study of plane turbulent wakes in a shallow water layer, Fluid Dynamics Research 16 (1995) 11–41.
[2] M.F. Tachie, B. Balachandar, Shallow wakes generated on smooth and rough surfaces, Experiments in Fluids 30 (2001) 467–474.
[3] V.H. Chu, S. Babarutsi, Confinement and bed-friction effects in shallow turbulent mixing layers, Journal of Hydraulic Engineering 114 (1988) 1257–1274.
[4] W.S.J. Uijttewaal, J. Tukker, Development of quasi two-dimensional structures in a shallow free-surface mixing layer, Experiments in Fluids 24 (3) (1998) 192–200.

[5] B. van Prooijen, W.S.J. Uijttewaal, A linear approach for the evolution of coherent structures in shallow Mixing Layers, accepted for publication in: Physics of Fluids, 2002
[6] H. Schlichting, Boundary-Layer Theory, McGraw Hill, New York, 1979.
[7] M. Giger, G.H. Jirka, T. Dracos, Entrainment and mixing in plane turbulent jets in shallow water, Journal of Hydraulic Research 29 (5) (1991) 615–642.
[8] R.J. Adrian, Particle-imaging techniques for experimental fluid mechanics, Annual Review of Fluid Mechanics 23 (1991) 261–304.
[9] M. Raffel, C. Willert, J. Kompenhans, Particle Image Velocimetrie, Springer Verlag, Berlin, 1998.
[10] L. Gui, W. Merzkirch, A comparative study of the MQD method and several correlation-based PIV evaluation algorithms, Experiments in Fluids 28 (2000) 36–44.
[11] F. Scarano, M.L. Riethmuller, Iterative multigrid approach in PIV image processing with discrete window offset, Experiments in Fluids 26 (1999) 513–523.
[12] J. Sheridan, J.C. Lin, D. Rockwell, Flow past a cylinder close to a free surface, Journal of Fluid Mechanics 330 (1997) 1–30.
[13] C.E. Willert, M. Gharib, The interaction of spatially modulated vortex pairs with free surfaces, Journal of Fluid Mechanics 345 (1997) 227–250.
[14] R.J. Adrian, C.D. Meinhart, C.D. Tomkins, Vortex organization in the outer region of the turbulent boundary layer, Journal of Fluid Mechanics 422 (2000) 1–54.
[15] P.F. Linden, B.M. Boubnov, S.B. Dalziel, Source-sink turbulence in a rotating stratified fluid, J. of Fluid Mech 298 (1995) 81–112.
[16] L. Tarbouriech, H. Didelle, D. Renouard, Time-series PIV measurements in a very large rotating tank, Experiments in Fluids 23 (1997) 438–440.
[17] W.S.J. Uijttewaal, Groyne field velocity patterns determined with particle tracking velocimetry, in: Proceedings 28th IAHR Congress, Graz, 1999.
[18] W.S.J. Uijttewaal, V. Weitbrecht, C.F.v. Carmer, G.H. Jirka, Experiments on shallow flow turbulence. in: Proceedings of the 3rd International Symposium on Environmental Hydraulics, Tempe, USA, 2001.
[19] C.F.v. Carmer, V. Weitbrecht, G.H. Jirka, On the genesis and fate of large coherent vortical structures in turbulent shallow wake flows, in: Proc. 3rd International Symposium on Environmental Hydraulics, Tempe, USA, 2001.
[20] J. Westerweel, Theoretical analysis of the measurement precisiion in particle image velocimetry, Experiments in Fluids 29 (7) (2000) 3–012.
[21] K. Nübel, V. Weitbrecht, Visualization of localization in grain skeletons with particle image velocimetry, accepted to be published in: Journal of Testing and Evaluation, ASTM, 2002 30(4) 322–328.
[22] I. Grant, Particle image velocimetry: a review, Proc. Institution of Mechanical Engineers 211 ((Part C)) (1997) 55–76.
[23] G. Kühn, PIV und PTV im Strömungslabor: Erfassung von Oberflächengeschwindigkeiten mit Ganzfeldmessverfahren, diploma thesis, Institute for Hydromechanics, University of Karlsruhe, Karlsruhe, Germany, 2000.
[24] V. Weitbrecht, G.H. Jirka, Flow patterns in dead zones of rivers and their effect on exchange processes, in: Proceedings of the 3rd International Symposium on Environmental Hydraulics, Tempe, USA, 2001.
[25] W.S.J. Uijttewaal, D. Lehmann, A. van Mazijk, Exchange processes between a river and its groyne fields: model experiments, Journal of Hydraulic Engineering 127 (11) (2001) 919–927.
[26] V. Weitbrecht, C. Hinterberger, Ergebnisse von physikalischen und numerischen experimenten an umströmten buhnenfeldern. from: “New insights in the physical and ecological processes in groyne fileds”, ISBN: 90-9015916-9, TU-Delft, The Netherlands, (2002) 63–77.
[27] D.J. Tritton, Physical Fluid Dynamics, Oxford University Press, New York, 1988.